Cross sections for the production of mass-6 and mass-7 nuclides in the proton-induced spallation of ^{20}Ne[†]

Lolo M. Panggabean,[*] Sam M. Austin, and Helmut Laumer

Cyclotron Laboratory and Physics Department, Michigan State University, East Lansing, Michigan 48824

(Received 26 June 1974)

Cross sections for proton-induced spallation of ^{20}Ne leading to nuclides with mass 6 or mass 7 were measured at proton energies between 30 and 40 MeV. Time-of-flight techniques were used for mass identification.

> NUCLEAR REACTIONS ^{20}Ne + p; E = 30.0, 35.0, 40.0 MeV; measured spallation
> σ for producing masses 6, 7; gas targets. Discuss astrophysical significance.

I. INTRODUCTION

Since ^{6}Li and ^{7}Li do not survive the hydrogen-burning stage in stars[1] and are not made in their observed abundance by primeval events,[2] it has become clear that these nuclides must be formed by $\alpha + \alpha$ reactions and by the proton- or α-induced spallation of heavier targets.[1-6] Reactions induced by the galactic cosmic rays appear to produce the required amount of ^{6}Li but too little ^{7}Li.[2] While a number of other reaction mechanisms can lead to ^{7}Li production,[2] it is still far from clear which of

these are possible or important. Whatever the detailed mechanism, however, measured cross sections for the relevant reactions are a necessary ingredient of a sound creation theory. Spallation cross sections for proton energies from threshold to 40 MeV and above are available for ^{12}C, ^{14}N, and ^{16}O (see Refs. 3, 7–10) but none exist for ^{20}Ne which is nearly as abundant as ^{14}N.

The measurements for ^{20}Ne presented in this paper are part of a program designed to provide spallation cross section measurements on astrophysically interesting targets at proton energies
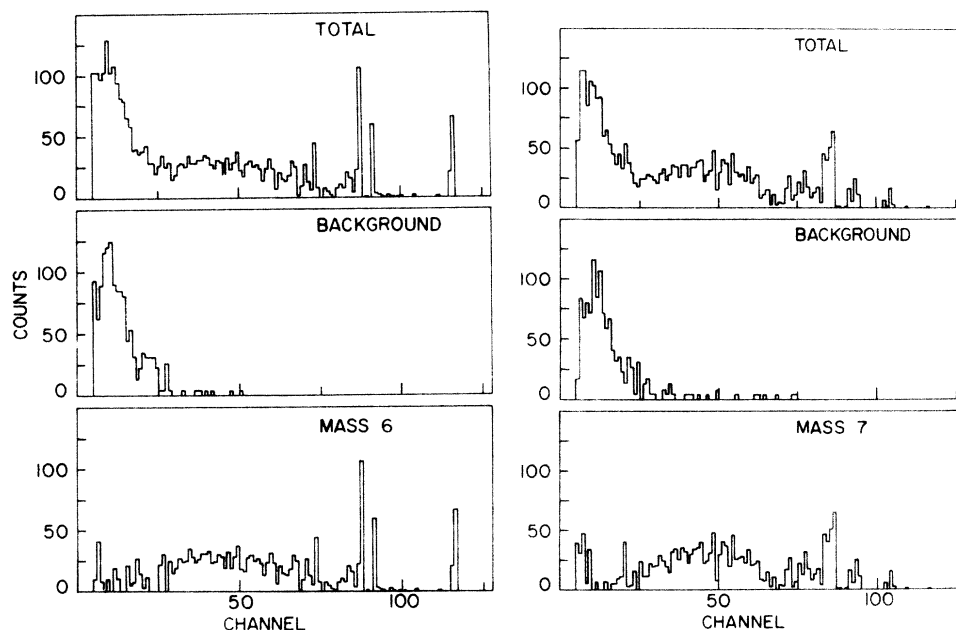

FIG. 1. Particle energy spectra at E_p = 40.0 MeV, θ_{lab} = 17°. These spectra were derived from a 128 channel × 128 channel array of Et^2 vs E by defining mass bands and projecting them on the E axis. Spectra for 42.0 Torr gas pressure (labeled TOTAL) and for 0.0 Torr gas pressure (labeled BACKGROUND) and their differences (labeled MASS 6 or MASS 7) are shown. The energy scale is 0.18 MeV/channel.
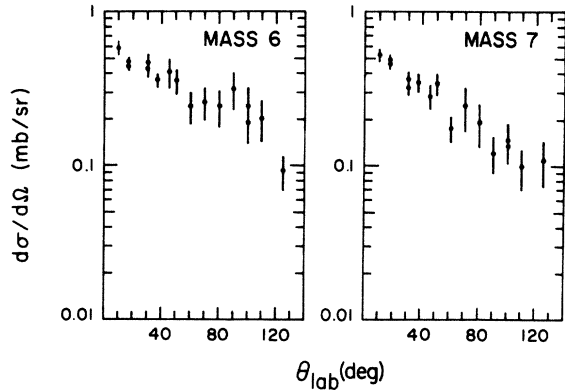
FIG. 2. Angular distributions at $E_p = 40.0$ MeV.

accessible to the Michigan State University (MSU) sector-focused cyclotron.

II. EXPERIMENTAL TECHNIQUE

The experimental method was essentially the same as previously described and further details, particularly of the extrapolation procedures discussed below, can be found in Refs. 8–10. Protons from the MSU sector-focused cyclotron, with an average burst width of 0.4–0.6 nsec, bombarded a gas target. A measurement of the flight time t required for a particle with mass m and energy E to cover a distance d yielded the mass m of the particle through the relationship $Et^2 = m(d^2/2)$. Although Et^2 yields only the mass m and not the charge of a particle, only one isobar of each mass is stable so that for many astrophysical purposes mass 6 can be identified with ^{6}Li and mass 7 with ^{7}Li.

The target gas, 99.66 mol% enriched ^{20}Ne, was confined in an ultra-thin-window[9] gas cell at a pressure between 23 Torr and 43 Torr. The collimation system was optimized[9] to restrict the region of origin of reaction products which were detected in an 86 or 150 μm thick silicon surface barrier detector 27 cm from the target. The flight time t was determined by starting a time-to-amplitude converter with a timing pulse derived from the detector E signal and stopping it with a signal obtained from the cyclotron radio frequency.

Angular distributions were measured at 30.0, 35.0, and 40.0 MeV. Data were taken under control of an XDS Sigma 7 computer and the MSU general purpose data acquisition code. The quantity Et^2 was calculated on line and displayed vs E in a 128 ×128 channel array. Mass bands appearing on this display were then processed to yield the energy spectra shown in Fig. 1. The low energy parts ($E < 4.5$ MeV) of the spectra were contaminated by background events probably due to neutron-induced reactions in the silicon detector. This background was more severe at higher proton beam energies. Background spectra taken with no gas in the cell allowed us to correct for this background in the case of mass 6 and 7. For masses 10 to 12 this could not be done with confidence, because the mass resolution was worse and the energy spectra contained few counts above 4.5 MeV. Consequently data are not presented for these nuclides.

To obtain the total cross section we integrated over particle energy at each angle and then over the total solid angle. Since the flight time available for particle identification is finite, ranging from 62 nsec at 30.0 MeV to 55 nsec at 40 MeV, the energy spectra all exhibit a low energy cutoff. The largest value of this cutoff was about 1 MeV for mass 7 at $E_p = 40$ MeV. An estimate of the yield below the energy cutoff of the spectra was based on an average of the last few nonzero channels in the low energy part of the spectra. A sample angular distribution is shown in Fig. 2. As a check on the sensitivity of the cross sections to the background subtraction, we also used an energy cutoff of 4.5 MeV with an extrapolation based on an average of counts in channels just above 4.5 MeV. The rather similar cross sections obtained by the two methods were averaged to yield those reported in Table I, retaining the larger of the two error assignments. This extrapolation and the extrapolation to unmeasured angles near 0 and 180° introduced the greatest uncertainties in the values of the measured cross sections. At each angle half of the contribution below the energy cutoff was assigned as error and was combined in quadrature with the statistical error of the yield.

These uncertainties were then summed linearly

TABLE I. Cross sections for mass 6 and 7 in ^{20}Ne proton spallation.

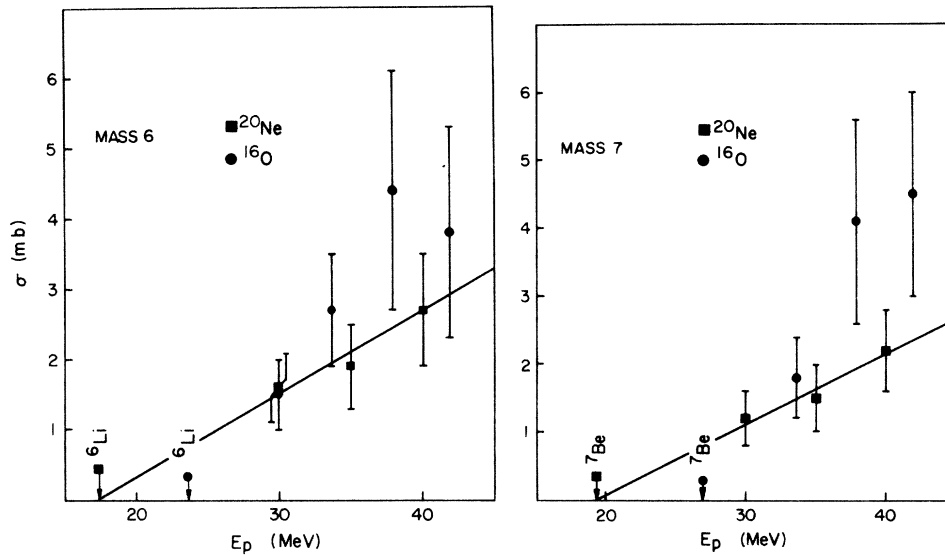| | ^{20}Ne(P,A) | | | | | |
| | $A = 6$ | | $A = 6$ | $A = 7$ | | $A = 7$ |
| | Energy cutoff | | | Energy cutoff | | |
E_p	Low	High	Average	Low	High	Average
30	1.6 ± 0.4	1.5 ± 0.5	1.6 ± 0.5	1.2 ± 0.3	1.2 ± 0.4	1.2 ± 0.4
35	1.7 ± 0.5	2.1 ± 0.6	1.9 ± 0.6	1.4 ± 0.4	1.6 ± 0.5	1.5 ± 0.5
40	2.4 ± 0.5	3.0 ± 0.8	2.7 ± 0.8	2.0 ± 0.5	2.4 ± 0.6	2.2 ± 0.6

FIG. 3. Production cross sections for masses 6 and 7 from proton spallation of ^{20}Ne compared to those of ^{16}O at similar energies (Ref. 10). Error bars represent total errors. The arrows on the abscissas show the location of the lowest threshold for each mass. The lines are linear least-squares fits to the ^{20}Ne points, the line being constrained to pass through the threshold point, and may be useful in forming analytic approximations to these cross sections. The slopes of these lines are 0.12 mb/MeV and 0.10 mb/MeV for mass and mass 7, respectively.

over angle and 0.5 of the yield extrapolation to un-measured back angles of the angular distribution plus 0.2 of the yield extrapolation to forward angles was also added linearly to obtain the total uncertainty. This linear addition was used in case all cutoff corrections were in error in the same direction; however, some mutual cancellation is likely and therefore, the quoted uncertainties are probably conservative. The uncertainties in detector solid angle, current integration, and gas density totaled about 3.3% and were generally negligible compared to the extrapolation errors. The cross sections are presented in Table I and are compared in Fig. 3 with those for mass 6 and 7 from spallation of ^{16}O at similar proton energies.

III. CONCLUSIONS

The ^{20}Ne cross sections shown in Fig. 3 contain no surprises. Had they increased more rapidly near threshold than a typical cross section, the importance of ^{20}Ne as a target would have been en-

hanced, since cosmic-ray fluxes are larger at low energies. As the cross sections in fact increase more slowly than those for ^{16}O, one expects the opposite effect; namely, that the contribution per ^{20}Ne target is somewhat less than that per ^{16}O target. This assumes of course that at high energies the cross sections become identical.[1]

While an accurate assessment of the importance of ^{20}Ne requires an extensive calculation on the scale of Refs. 3, 5, and 6, an indication of the size of its contribution can be obtained by assuming that the ^{16}O and ^{20}Ne cross sections differ only slightly. The ratio of production from ^{16}O and ^{20}Ne will then be given roughly by the ratio of their abundances in the cosmic rays or in the interstellar medium which is ^{16}O : ^{20}Ne $\simeq 4$–5.[3] Thus we expect the contribution of ^{20}Ne to be about 20–25% that of ^{16}O or based on Mitler's calculation,[5] about 5% of the over-all ^{6}Li production and 4% of the over-all ^{7}Li production. Thus, while this contribution is large enough to be included, it need not be calculated accurately.

[1]R. Bernas, E. Gradsztajn, H. Reeves, and E. Schatzman, Ann. Phys. (N. Y.) 44, 426 (1967).
[2]H. Reeves, J. Audouze, W. A. Fowler, and D. N.
Schramm, Astrophys. J. 179, 909 (1973).
[3]M. Meneguzzi, J. Audouze, and H. Reeves, Astron. Astrophys. 15, 337 (1971).
[4]H. Reeves, W. A. Fowler, and F. Hoyle, Nature (Lond.) 226, 727 (1970).
[5]H. E. Mitler, Astrophys. Space Sci. 17, 186 (1972).
[6]J. Audouze and J. W. Truran, Astrophys. J. 182, 839

(1973).

[7]F. Yiou, C. Seide, and R. Bernas, J. Geophys. Res. <u>74</u>, 2447 (1969).

[8]C. N. Davids, H. Laumer, and S. M. Austin, Phys. Rev. C <u>1</u>, 270 (1970); Phys. Rev. Lett. <u>23</u>, 1388

(1969).

[9]H. Laumer, S. M. Austin, L. M. Panggabean, and C. N. Davids, Phys. Rev. C <u>8</u>, 483 (1973).

[10]H. Laumer, S. M. Austin, and L. M. Panggabean, unpublished.